

Supplement of Atmos. Chem. Phys., 20, 10231–10258, 2020
<https://doi.org/10.5194/acp-20-10231-2020-supplement>
© Author(s) 2020. This work is distributed under
the Creative Commons Attribution 4.0 License.



Supplement of

A global model–measurement evaluation of particle light scattering coefficients at elevated relative humidity

María A. Burgos et al.

Correspondence to: María A. Burgos (maria.burgos@aces.su.se) and Paul Zieger (paul.zieger@aces.su.se)

The copyright of individual parts of the supplement might differ from the CC BY 4.0 License.

Figure S1 shows the location of the in situ measurement sites used in this study. The black dot on the background represent the actual latitude, longitude coordinates, while the small colored stars represent the closest grid point given by each model. The site ID has been color-coded by site type following the description used throughout the manuscript: blue for Arctic sites (BRW and ZEP), cyan for marine (CBG, GRW, GSN, MHD, PVC, PYE, and THD), dark green for mountain (JFJ), light green for rural (APP, CES, FKB, HLM, HYY, LAN, MEL, and SGP), black for urban (HFE, PGH, and UGR), and red for desert (NIM).

5 Figure S2 presents the probability density function of the measured RH_{ref} for all sites. While some sites are clearly below the recommended threshold of $RH_{ref} < 40\%$, some sites clearly exceed the recommended RH threshold given by WMO/GAW (2016). The measurement data with $RH_{ref} > 40\%$ were not considered in this study. This figure also shows the broad distribution of RH_{ref} at some sites, where control of the DryNeph sampling conditions was problematic.

10 Figure S3 shows the annual cycle of $f(RH=85\% / RH=40\%)$ at Southern Great Plains for the whole period of measurements (1999-2016) with the black line representing the monthly median values and the gray shading representing the interquartile range for all measurements. The monthly median values for each individual year are showed with gray lines. The year 2010 is shown in red (2010 is the year that is compared to model outputs). A threshold of more than 10 data points per month has been required to minimize the influence of possible outliers on the monthly values. This figure gives an idea of the possible

15 impact of considering different years in the model-measurement comparison. The years showing largest differences with the climatological average values are 2004, 2005, and 2006, with the largest differences found in May (63.2%, 62%, and 67%, respectively) and September (52%, 85.3%, and 65.5%, respectively). In contrast, the average difference (over the 18 years considered in SGP) for a given month between a single year and the climatological average, varies between 11 (January) and 23% (May).

20 Figure S4 shows the mass mixing ratio of the chemical components simulated by the ten models in this study: black carbon(bc), dust, organic aerosol (oa), sulfates (so4), sea salt (ss), nitrate (no3), and ammonium (nh4). This data has been collocated for those months with $f(RH)$ measurements at each of the 22 sites considered.

Figures S5, S6, and S7 show the annual cycle for the year 2010 of the mass mixing ratio (%) at BRW, GRW, and SGP for the ten models in this study.

25 Figure S8 shows the annual cycle of $f(RH=85\%/RH_{ref}=40\%)$, $f(RH=85\%/RH_{ref}=0\%)$, and $f(RH=40\%/RH_{ref}=0\%)$ at BRW, GRW, and SGP for the ten models in this study.

Figure S9 shows the scattering enhancement vs. relative humidity for different aerosol types measured at various European sites using a tandem nephelometer humidograph system

Figure S10 illustrates the scattering enhancement between 0 and 40% (i.e., $f(RH=40\%/RH=0\%)$) as calculated by the models

30 in this study.

Figure S11 presents the probability density function of $f(RH=85\%)$ when RH_{ref} is set to 40% or RH_{ref} is taken at the driest measured RH (value between 0-40%, see Fig. S2).

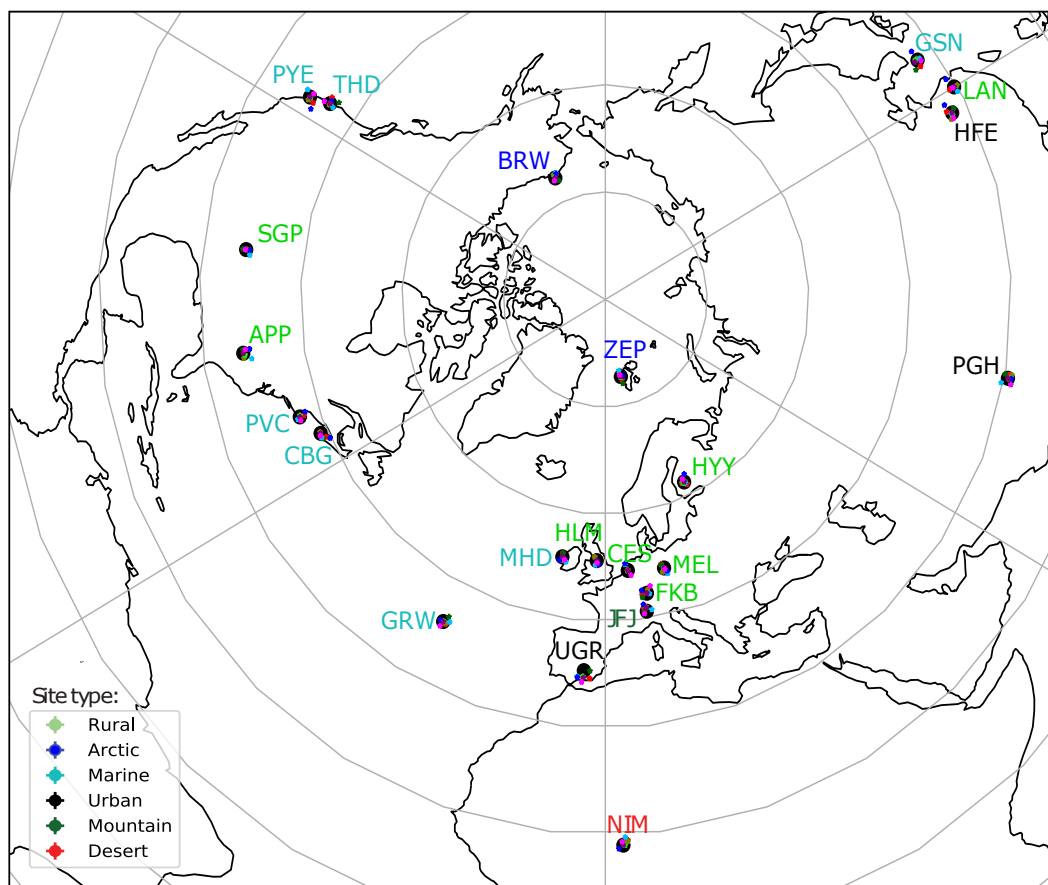


Figure S1. Location of the 22 in situ measurement sites (latitude, longitude coordinates in black circles and closest model grid point in colored stars) used in this study, with the site ID color-coded by site type. Station acronyms are given in Table 1 in the main manuscript.

References

WMO/GAW: WMO/GAW Aerosol Measurement Procedures, Guidelines and Recommendations, Report No. 227, World Meteorological Organization, Geneva, Switzerland, 2nd edition edn., 2016.

- 5 Zieger, P., Fierz-Schmidhauser, R., Weingartner, E., and Baltensperger, U.: Effects of relative humidity on aerosol light scattering: results from different European sites, *Atmos. Chem. Phys.*, 13, 10 609–10 631, <https://doi.org/10.5194/acp-13-10609-2013>, <http://www.atmos-chem-phys.net/13/10609/2013/>, 2013.

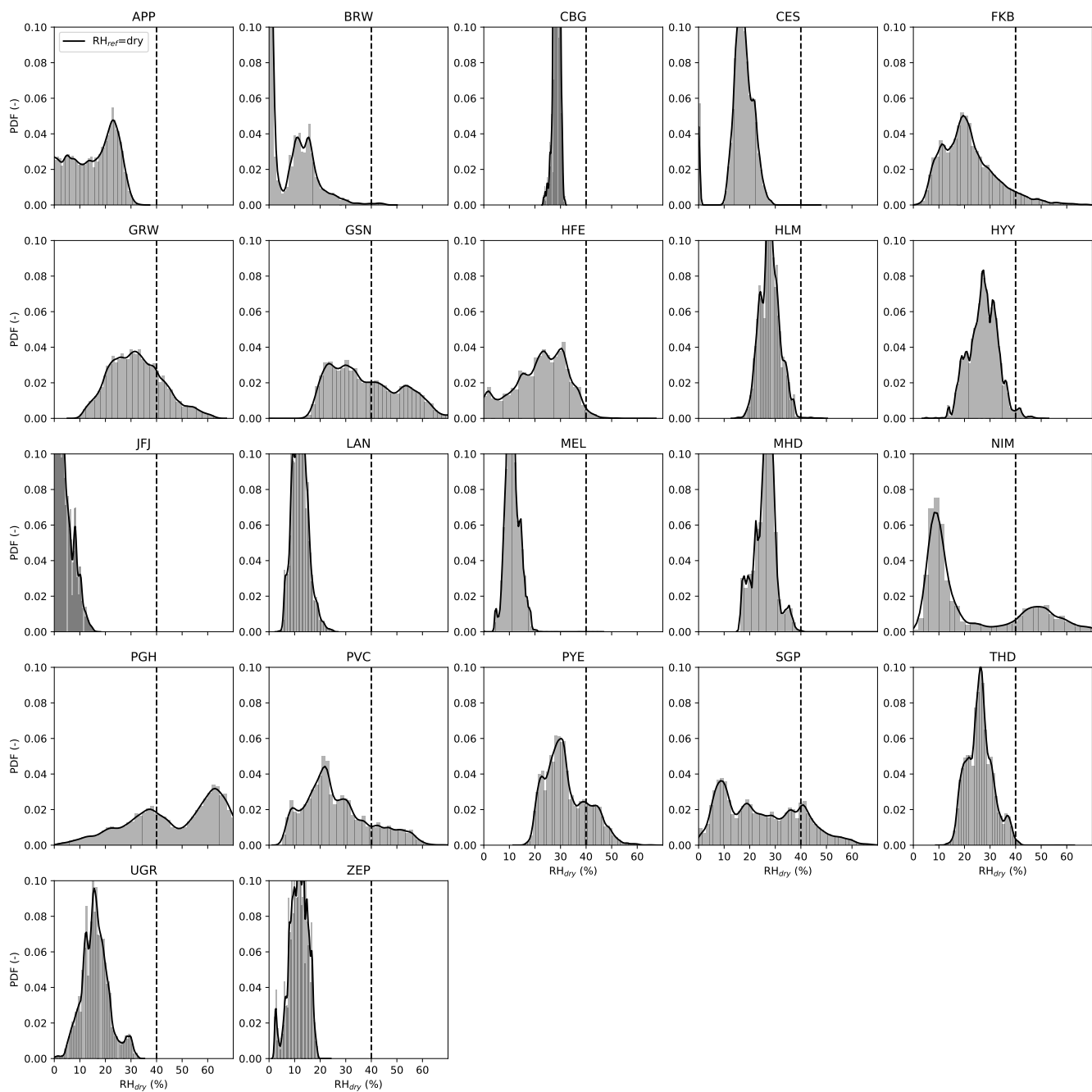


Figure S2. Probability density function of RH inside the dry nephelometer for all measurement sites used in this study. The recommended threshold for in situ sampling below 40 % RH is marked by a dashed line (WMO/GAW, 2016). Station acronyms are given in Table 1 in the main manuscript.

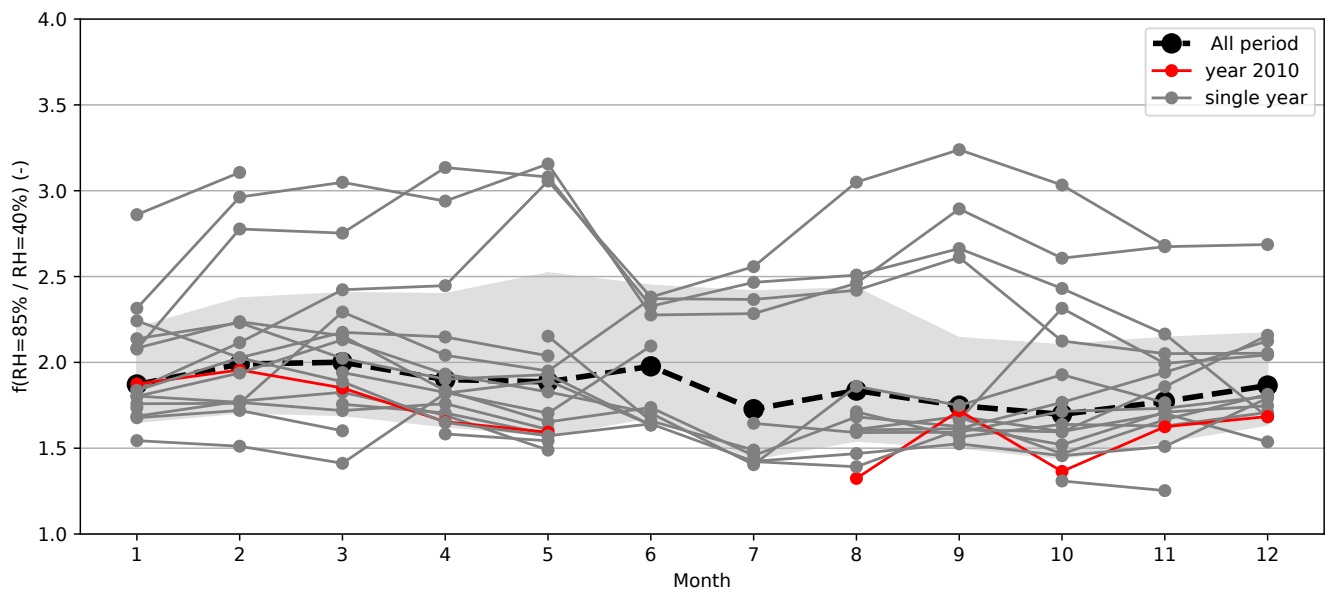


Figure S3. Annual cycles of the median $f(\text{RH}=85\% / \text{RH}_{\text{ref}}=40\%)$ for the whole measurement period at SGP (1999 to 2016, dashed black line) and median values for each individual year (gray lines). Median values for the year 2010 are represented by a red line (2010 is the year which is compared to model output). The shaded gray area represents the interquartile range of all measurements.

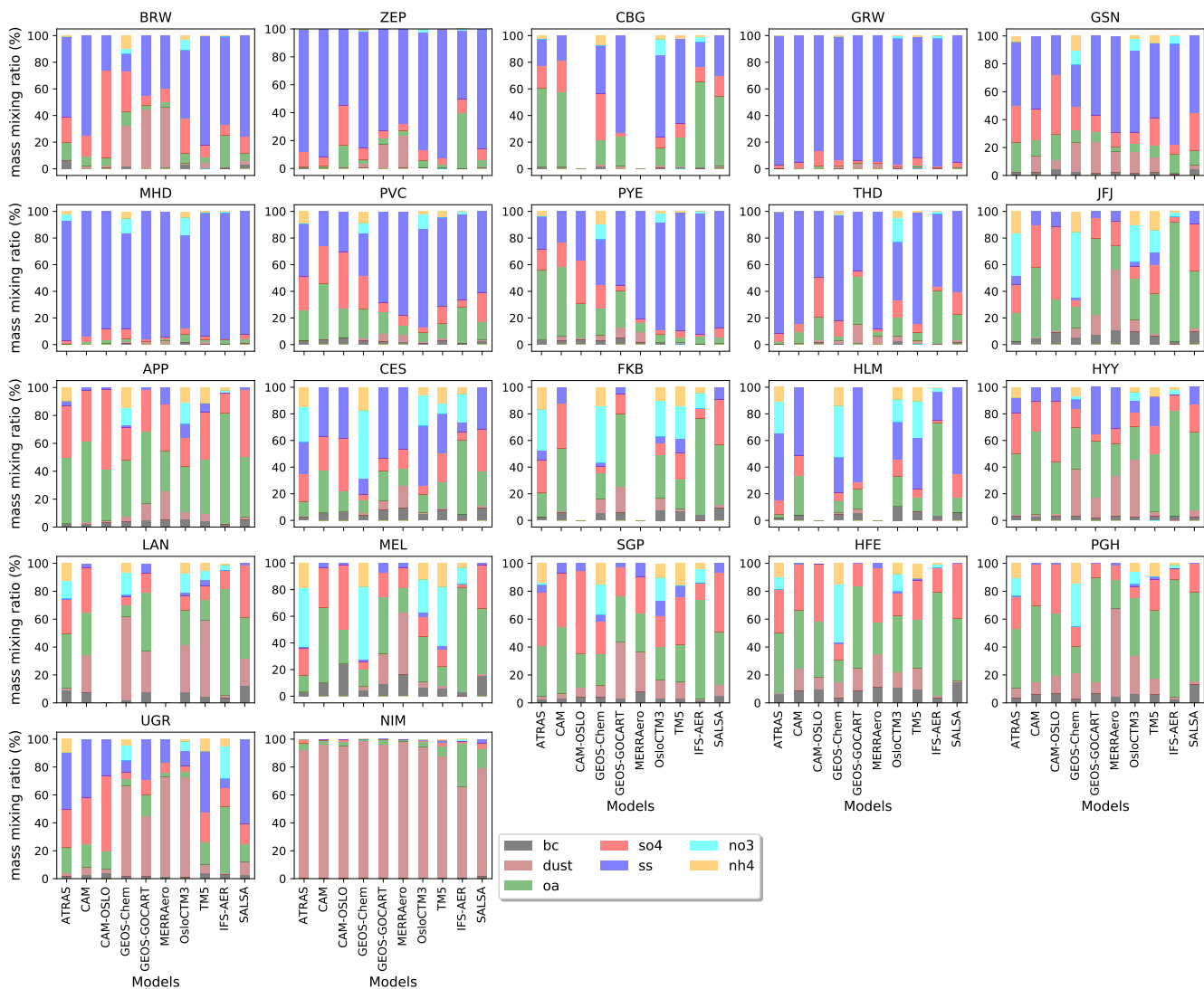


Figure S4. Mass mixing ratio (%) of black carbon (bc), desert dust (dust), organic aerosol (oa), sulfates (so4), sea salt (ss), nitrate (no3), and ammonium (nh4) for the ten models used in this study, collocated for those months with $f(\text{RH})$ measurements at each of the 22 sites considered. New Figure.

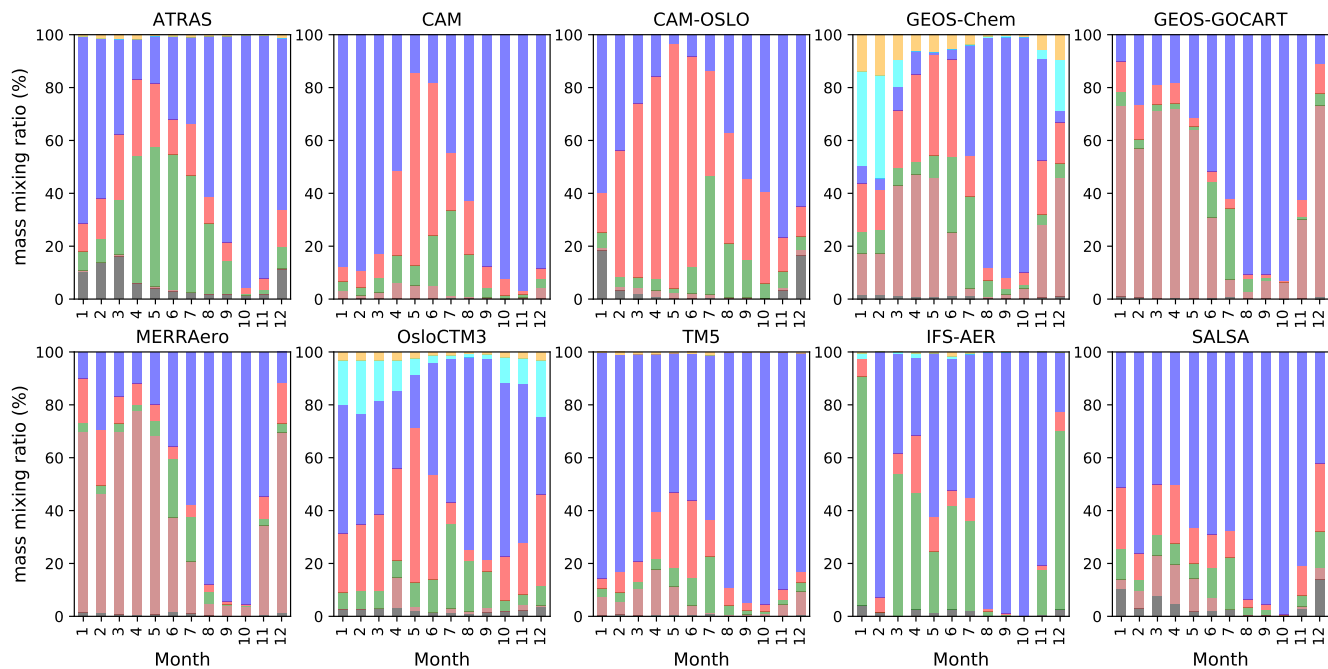


Figure S5. Annual cycle of the mass mixing ratio (%) at BRW for each model. See Fig. S4 for legend. New Figure.

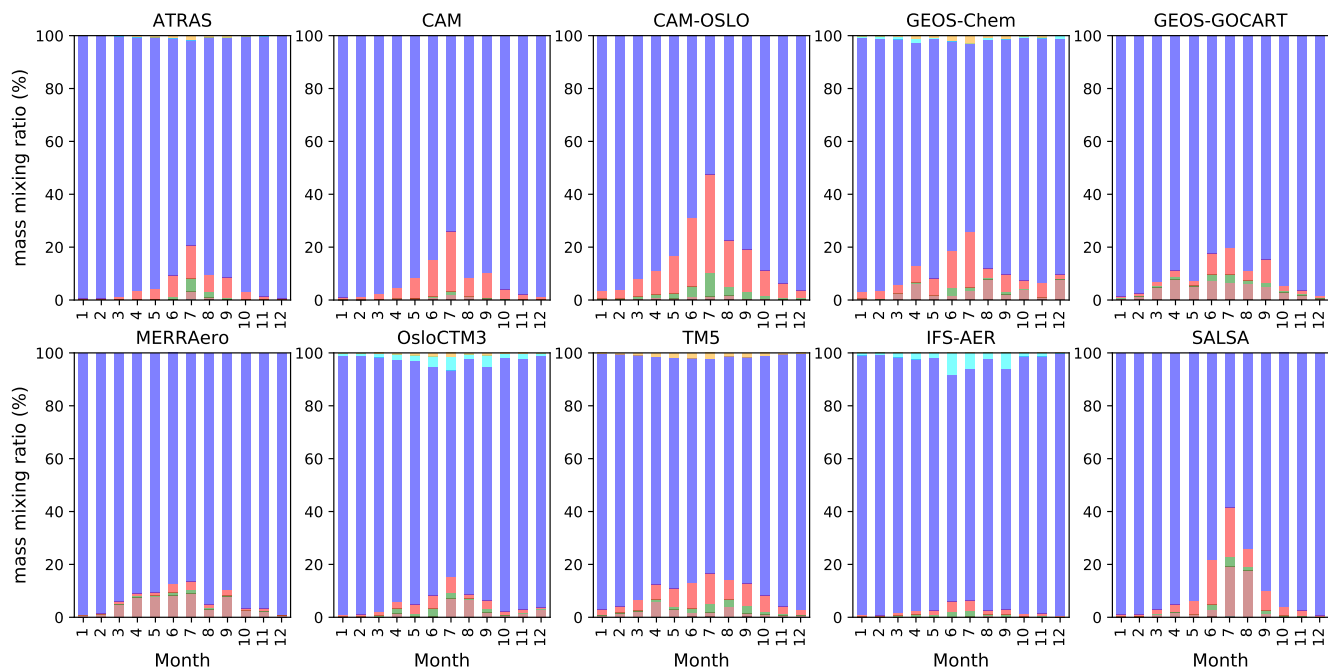


Figure S6. Annual cycle of the mass mixing ratio (%) at GRW for each model. See Fig. S4 for legend. New Figure.

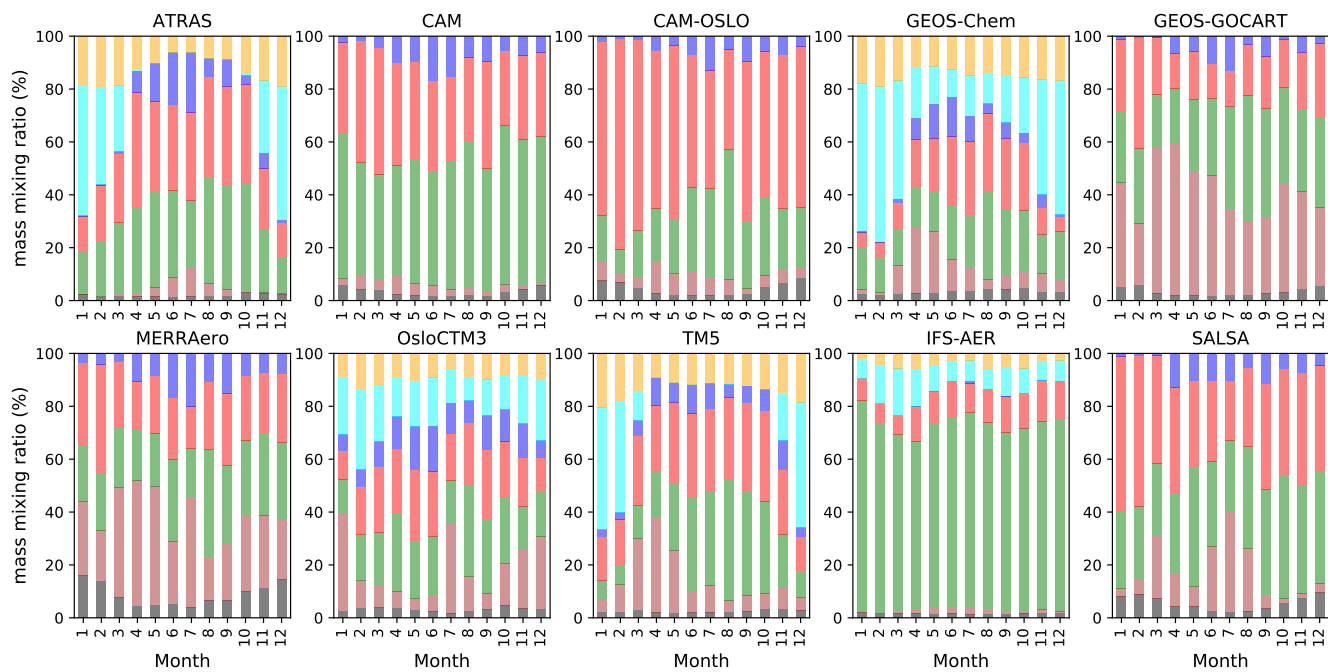


Figure S7. Annual cycle of the mass mixing ratio (%) at SGP for each model. See Fig. S4 for legend. New Figure.

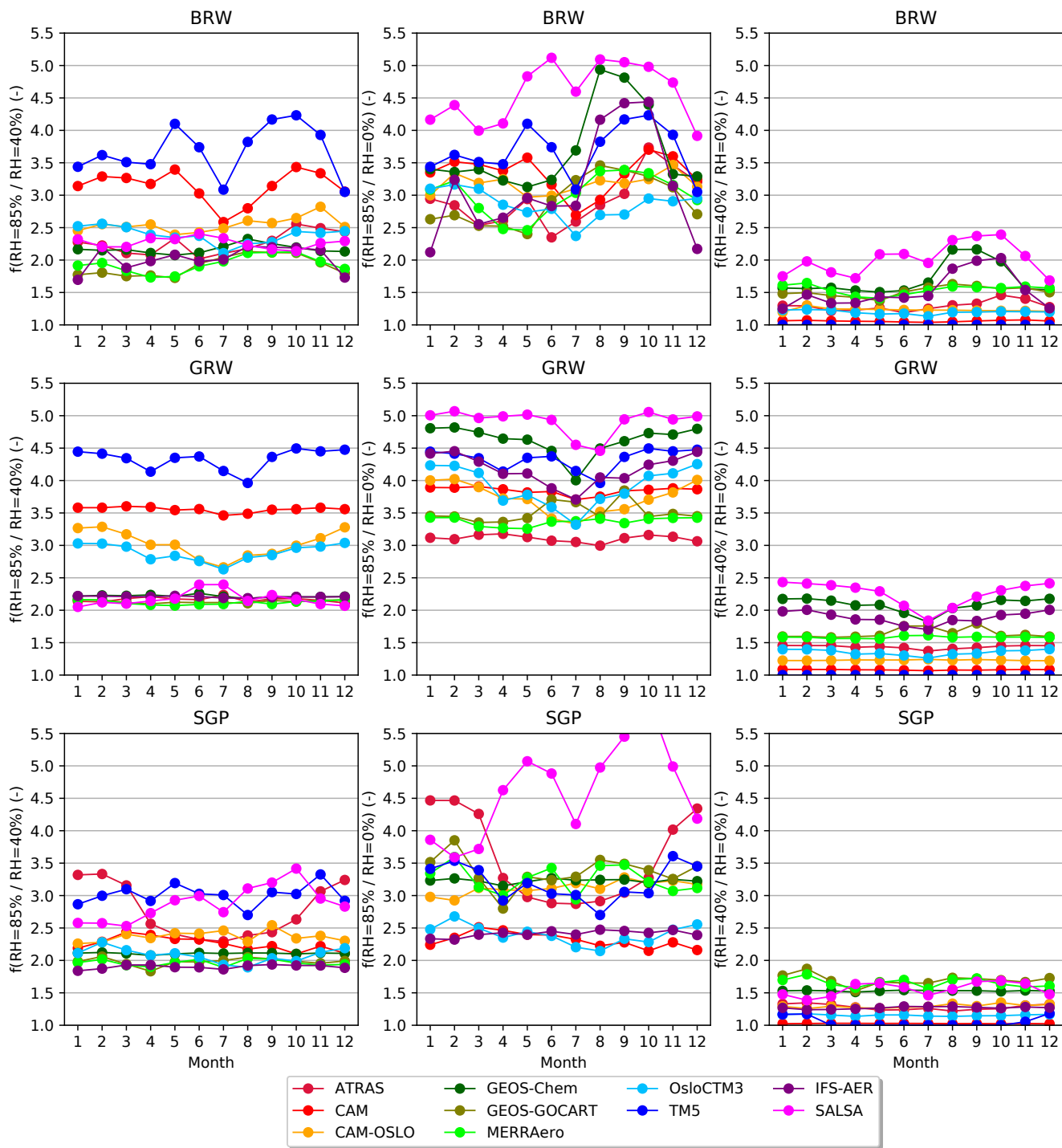


Figure S8. Annual cycle of median $f(\text{RH}=85\% / \text{RH}=40\%)$ (left column of plots), $f(\text{RH}=85\% / \text{RH}=0\%)$ (middle column of plots), and $f(\text{RH}=40\% / \text{RH}=0\%)$ (right column of plots) for all models at BRW, GRW, and SGP. New Figure.

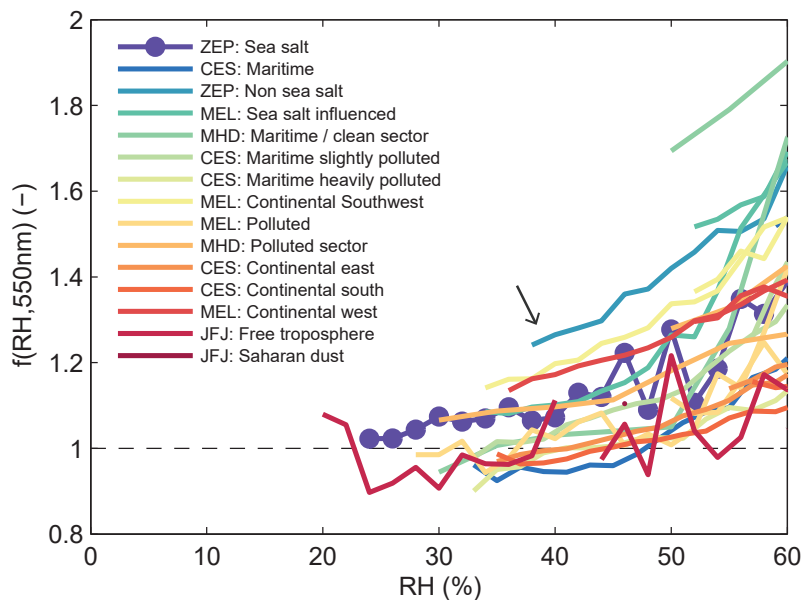


Figure S9. Scattering enhancement vs. relative humidity for different aerosol types measured at various European sites using a tandem nephelometer humidograph system (taken from Zieger et al., 2013). Lines are color coded from clean/maritime air masses (blue lines) to polluted/dust air masses (red lines). The curve for the pristine sea salt dominated event measured at Ny-Ålesund, in the Arctic (blue dots), follows the behavior of pure inorganic sea salt, which would also exhibit hysteresis effects. Figure moved from main text to supplementary.

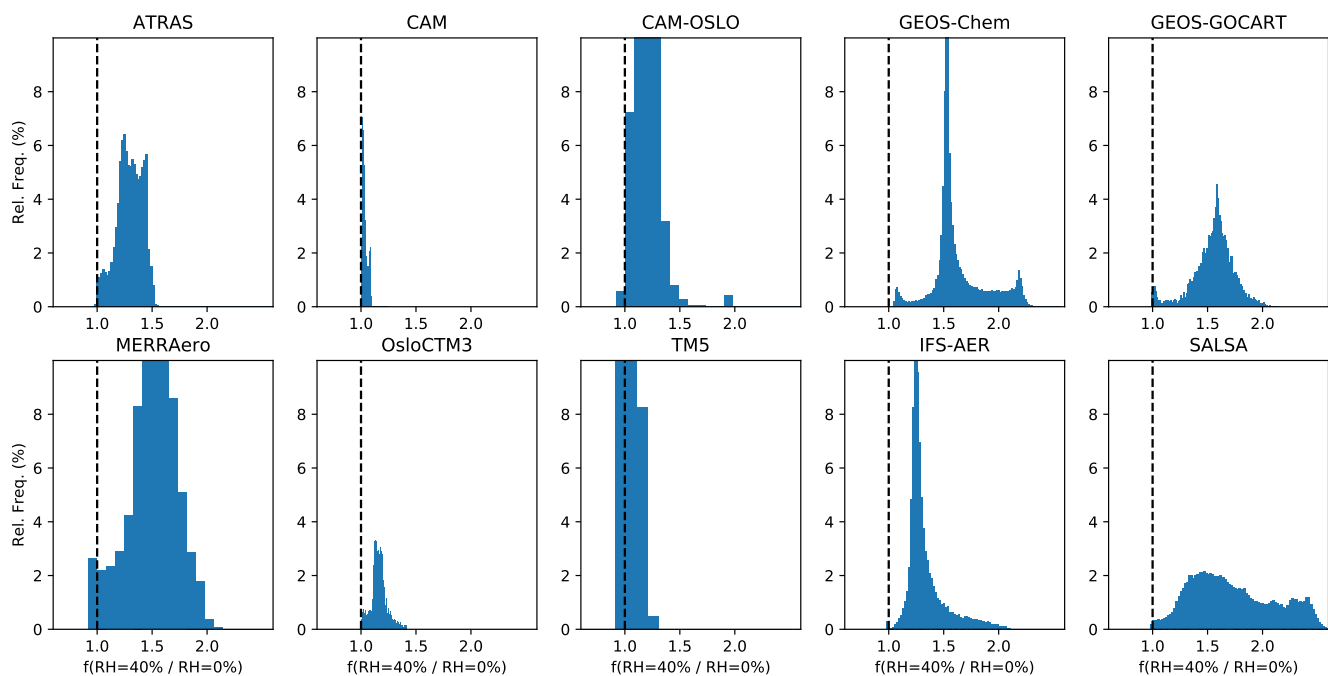


Figure S10. Relative frequency of occurrence (%) of the modeled scattering enhancement between 0 and 40 % RH ($f(\text{RH}=40\%/\text{RH}=0\%)$) calculated by the models for all sites considered in this study. The dashed black line marks the value of no change in $f(\text{RH})$ between 0 and 40 % RH. The y-axis for CAM-OSLO, MERRAero, TM5 and IFS-AER is kept to a maximum of 10 for illustrative purposes.

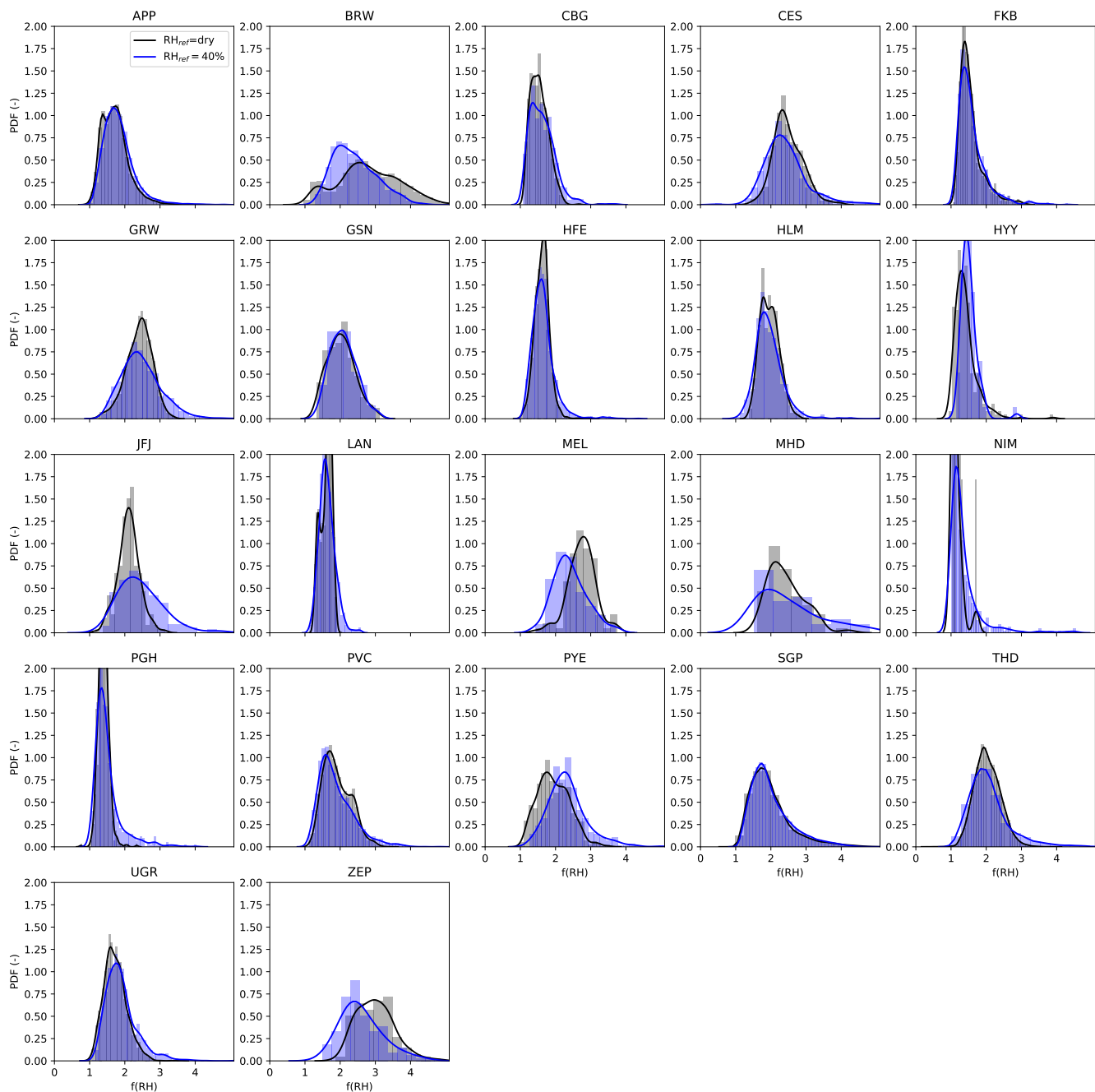


Figure S11. Probability density function of the measured $f(\text{RH}=85\%)$ for $\text{RH}_{\text{ref}} = 40\%$ (blue) and $\text{RH}_{\text{ref}} = \text{dry}$ (values below 0-40%, see Fig. S2; gray) for all sites used in this study. Station acronyms are given in Table 1 in the main manuscript.